

# Development of Broadband Radar and Initial Observation

Tomoo Ushio, Kazushi Monden, Tomoaki Mega, Ken'ichi Okamoto and Zen-Ichiro Kawasaki

Dept. of Aerospace Engineering  
Osaka Prefecture University  
Osaka, Japan  
ushio@aero.osakafu-u.ac.jp

**Abstract**— We have developed a broad-band radar which is the precipitation Ku-band doppler radar using the pulse compression technique (bandwidth=80MHz), and observed the rainfall. We could successfully obtain the vertical profile of the equivalent reflectivity factor  $Z_e$  and doppler velocity with the high range-resolution from low altitude.

## I. INTRODUCTION

Rainfall observations using the weather radar have a great advantage in the point that it is possible to observe precipitation widely in the short time. However, the rainfall rate obtained from the weather radar doesn't necessarily correspond to that from the observation equipment on the ground such as rain-gauge. One of the causes of this disagreement is the beamfilling error. This error caused by the nonuniform of raindrop in the pulse volume. The other cause is that the most radar cannot obtain the echo from rainfall at low altitude, because that the using antenna is monostatic and the transmitted power is very high. Therefore, the horizontal moving of the rainfall at low altitude cannot be accurately obtained the reflectivity factor on the ground.

For the accurate estimation of rainrate on the ground using the weather radar, the weather radar should be the high range-resolution and be able to observe from low altitude.

In this study, we have developed the broad-band radar (Ku-band) which can transmit and receive the wideband (80MHz) signals and has bistatic antenna. Our radar uses the digital pulse compression technique, which is that we spread the transmitted pulse out in time and then processes the received echo with a matched filter to dispread it, therefore, we can acquire the rainfall profiles of high range-resolution and high SNR.

The pulse compression technique has the advantage that the high range-resolution profiles can be acquired by the low transmitted power. However, we might estimate the inaccurate rainrate by the range-sidelobe caused from this technique. For overcoming the disadvantage, we adopted Arbitrary Waveform Generator (AWG) for the signal source of our radar system and directly acquired the IF signal by the A/D converter (400MS/s, 12bit), then we can flexibly choose the transmitted waveform that the range sidelobe is suppressed enough and process the

pulse compression on the analysis software. In this paper, we adopted the chirp signal with the Blackman-Harris window function for the suppression of the range sidelobe. [1]

We observed the rainfall in our campus using the broad-band radar, then acquired the profile of the reflectivity factor from about 40m to a few km with the 4m range-resolution. In addition, the observed  $Z_e$  at 40m by the broadband radar corresponded well to the  $Z_e$  of the disdrometer on the ground.

Section II provides a description of the broad-band radar. In Section III, the results of the rainfall observation and the comparison with the measuring data from the other measuring equipments are shown.

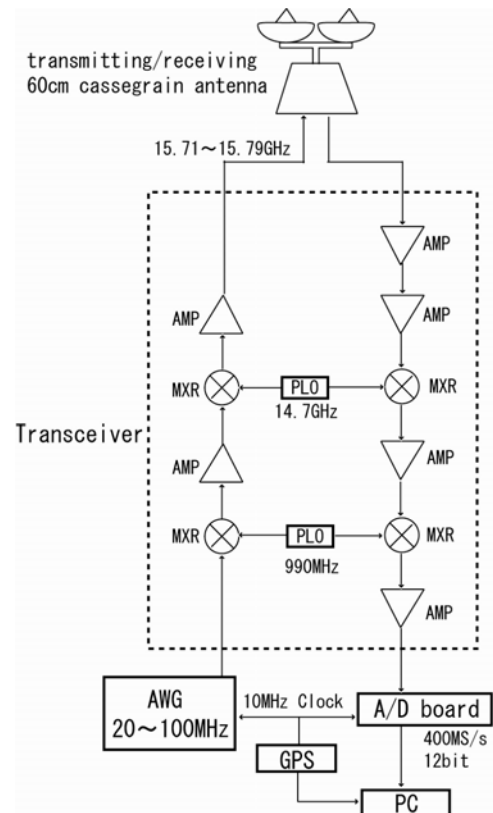


Figure 1. Block diagram of broad-band radar system

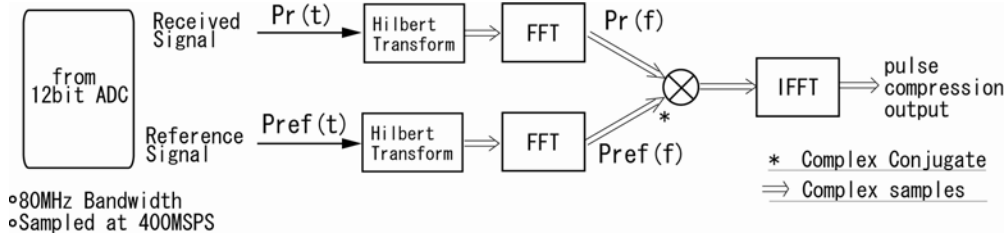


Figure 2. Flow of pulse compression process

## II. DESCRIPTION OF BROAD-BAND RADAR

### A. Configuration of Broad-band radar

A block diagram of the broad-band radar system is shown in Fig.1. This system consists of Arbitrary Waveform Generator (AWG), transceiver, transmitting/receiving casegrain type antennas (diameter=60cm), A/D converter and GPS. The chirp signal in the 20-100MHz frequency range, that pulsewidth is 128 $\mu$ s, is generated by the AWG, then the double phase lock oscillators in the transceiver upconverts this output to 15.71- 15.79GHz, and this output is amplified to about 100mW.

The received echo from the precipitation is down-converted to IF signal in the transceiver, then the signal is sampled by A/D converter (Sampling ratio: 400MS/s, Vertical resolution: 12bit, Available memory: 4Msamples) and saved to the PC. The high precision 10MHz reference clock from the GPS receiver is used for synchronizing the internal clock of the AWG and the A/D converter, and the GPS clock is used for the clock synchronization between the PC of the broad-band radar and of the other observation equipment, such as the disdrometer.

### B. Procedure of Data Processing

The flow chart of the pulse compression process in this study is shown Fig.2. In the pulse compression processing, we processed the cross-correlation between the received signal from the precipitation and the reference signal. The reference signal was pre-sampled in the state of directly connecting the transceiver output of the transmitting end to the input of the receiving end through the attenuator. In the cross-correlation, we processed in frequency domain by the FFT. The output of the pulse compression processing  $P_{pc}(t)$  is defined as

$$P_{pc}(t) = FFT^{-1}[P_r(f) \cdot P_{ref}^*(f)] \quad (1)$$

where  $P_{ref}^*(f)$ , which is called the matched filter, is the complex conjugate of  $P_{ref}(f)$ , and  $FFT^{-1}$  is the processing of the inverse fast Fourier transform. Before the received/reference signals was processed by FFT, the both real

data was converted to the complex data consist of the in-phase (I) and quadrature (Q) components using the Hilbert transform, in fact the I component is the real data from the A/D converter and the Q component is the Hilbert transformed data of it.

For estimating the doppler velocity of the raindrop, the successive data after the pulse compression in the same range bin was processed by FFT. In this observation, the pulse repetition frequency was about 6.8kHz and the number of pulses of FFT was 64.

### C. Range-resolution of Broad-band Radar

The typically pulse compressed waveform is written as

$$f(t) = \sqrt{TB} \frac{\sin(\pi BT)}{\pi BT} \quad (2)$$

where T is the pulsewidth, B is the bandwidth, and the mainlobe width of the waveform is 1/B. Therefore, the ideal range-resolution of the radar using the pulse compression can be written as

$$\Delta t = \frac{c}{2B} \quad (3)$$

where c is the velocity of light, and the range-resolution of our radar that bandwidth is 80MHz is about 1.9m.

However, the output waveform of the signal source (AWG) is the chirp signal that Blackman-Harris window function was multiplied, as a result, the range sidelobe is suppressed, but the mainlobe width broadens and so the range resolution degrades. If the signal with the window function is transmitted, the range resolution is about 4m. This result was made sure by the scattering experiment using this radar for a few metal plates as targets.

## III. RESULTS OF OBSERVATION

In this section, the results of the rainfall measuring and the comparison with the equivalent reflectivity factor Ze from the

disdrometer, which is the measurement instrument of the dropsize distribution on the ground, are provided. The values of the broad-band radar for the comparison are the  $Z_m$ , which is the equivalent reflectivity factor with the rainfall attenuation. [2] In comparing with the  $Z_e$  (disdrometer), the  $Z_m$  of the broad-band radar at 40m height, so this is the minimum height in the useful data, and 1-min mean values (the average of 30 data) are used.

Fig. 3 is a view showing a frame format of transmitting signals. The characteristics of the broad-band radar is shown TABLE I. A 2-sec resolution data is obtained from the 64 pulses data by the incoherent integration.

The installation location of the broad-band radar is in the campus of the Osaka Prefecture Univ., Osaka Japan, then the observation date is September 21, 2004.

In Fig. 4, the scatter plot of the  $Z_m$  from the broad-band radar and the  $Z_e$  from the disdrometer is shown, and the time series of the  $Z_m$  and the  $Z_e$  at 1-min mean values are shown in Fig. 5.

It has been understood that the both data are corresponding well from Fig. 4 and Fig. 5. In addition, the correlation coefficient is 0.98, and from this, it is shown that we accurately observed the rainfall.

The vertical  $Z_m$  profile of the broad-band radar with 2-sec resolution is shown in Fig. 6, and the magnified figure of Fig. 6 is shown in Fig. 7. Note that the developed broad-band radar is capable of observing the scattering signals from rain drops within the pulse volume with very high resolution and accuracy. The radar will be useful equipment to research on the fine structure in rainfall.

In order to compare our result with the conventional radar, the result from the Micro Rain Radar (METEK) which is located 2 meters apart from the broadband radar is shown in Figure 8 for the same rain event. The overall structure shows quite similar pattern with these two radars and the lower reflectivity was observed by the micro rain radar system. Although our broad band radar cannot observe the reflectivity below 20 dBz, the much finer resolution is achieved and the detailed structure of the rain event is clearly shown in contrast to that from the conventional radar system.

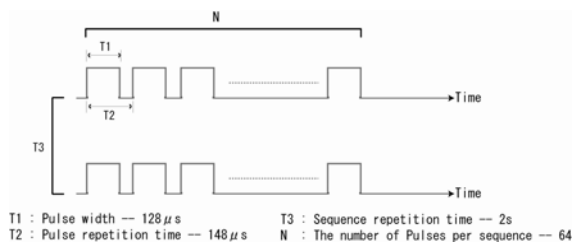


Figure 3. Sequence of transmitted pulse

TABLE I. OPERATING CHARACTERISTICS OF BROAD-BAND RADAR

<b>Pulse width</b>	<b>128 <math>\mu</math>s</b>
<b>Transmitted frequency</b>	<b>15.75GHz <math>\pm</math> 40MHz</b>
<b>Bandwidth</b>	<b>80MHz</b>
<b>Transmitted power</b>	<b>100mW</b>
<b>Beam width</b>	<b>2 degree</b>
<b>Antenna gain</b>	<b>32dB</b>
<b>Time resolution</b>	<b>2 sec</b>

#### IV. CONCLUSIONS

In this study, we developed the broad-band radar, and showed the initial evaluation. The observation using this radar shows that the detailed structure of rainfall was successfully acquired with the 4m range resolution, and the correlation coefficient between the  $Z_e$  of this radar at 40m in altitude and that of the disdrometer is shown to be 0.98.

In the future, we will develop the antenna rotating mechanism, and observe the rainfall by the volume of scan. So, the high time-resolution broad-band radar, which takes as long as 1 minute during the scan of the whole sky, will be develop using the fast scanning technique. [3]

#### REFERENCES

- [1] A. Y. Nashashibi, K. Sarabandi, P. Frantzis, R. D. De Roo and F. T. Ulaby, *An Ultrafast Wide-Band Millimeter-Wave(MMW) Polarimetric Radar for Remote Sensing Application*, IEEE Trans. Geosci. Remote Sensing, vol.40, NO.8, pp.1777-1786, August 2002.
- [2] Richard J. Doviak and Dušan S. Zrnić, *Doppler Radar and Weather Observation*, 2nd edition, San Diego, CA, Academic Press, 1993.
- [3] Paul R. Krehbiel and Marx Brook, *A Broad-Band Noise Technique for Fast-Scanning Radar Observations of Clouds and Clutter Targets*, IEEE Trans. Geosci. Electron., vol. GE-17, NO.4, pp.196-204, October 1979.

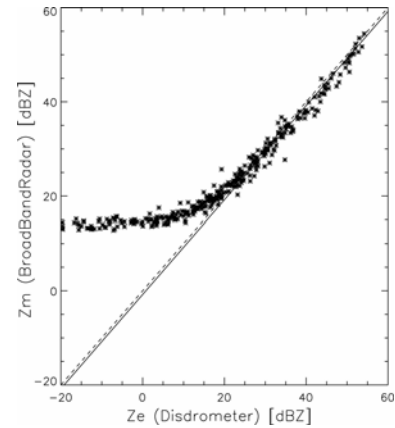


Figure 4. Scatter plot of the  $Z_m$  from the broad-band radar and the  $Z_e$  from the disdrometer. The solid line represents a linear regression of the data, while the dashed line represents a 1:1 slope.

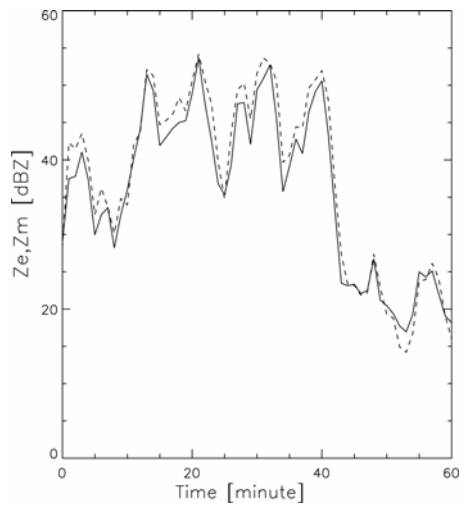


Figure 5. Time series graph of the Zm and the Ze (1-min mean values). The solid line is the Zm from the broad-band radar and the dashed line is the Ze from the disdrometer.

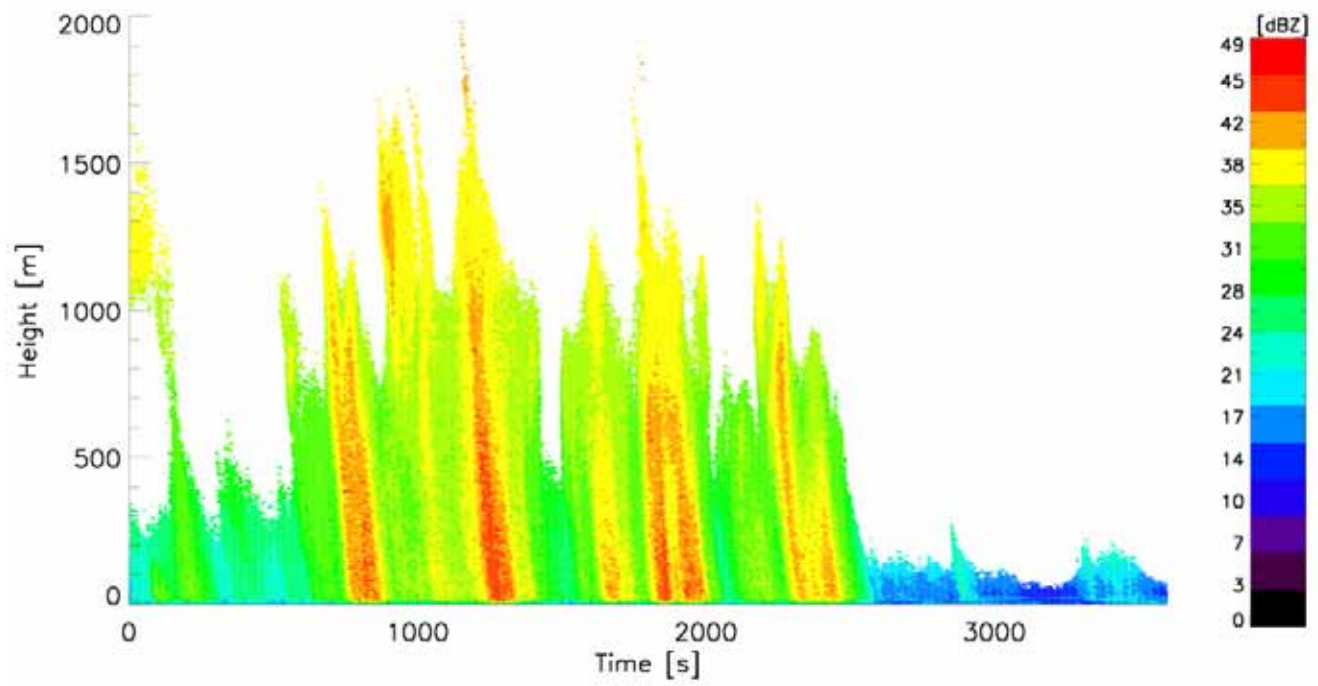


Figure 6. Vertical Zm profile of broad-band radar with 2-sec resolution

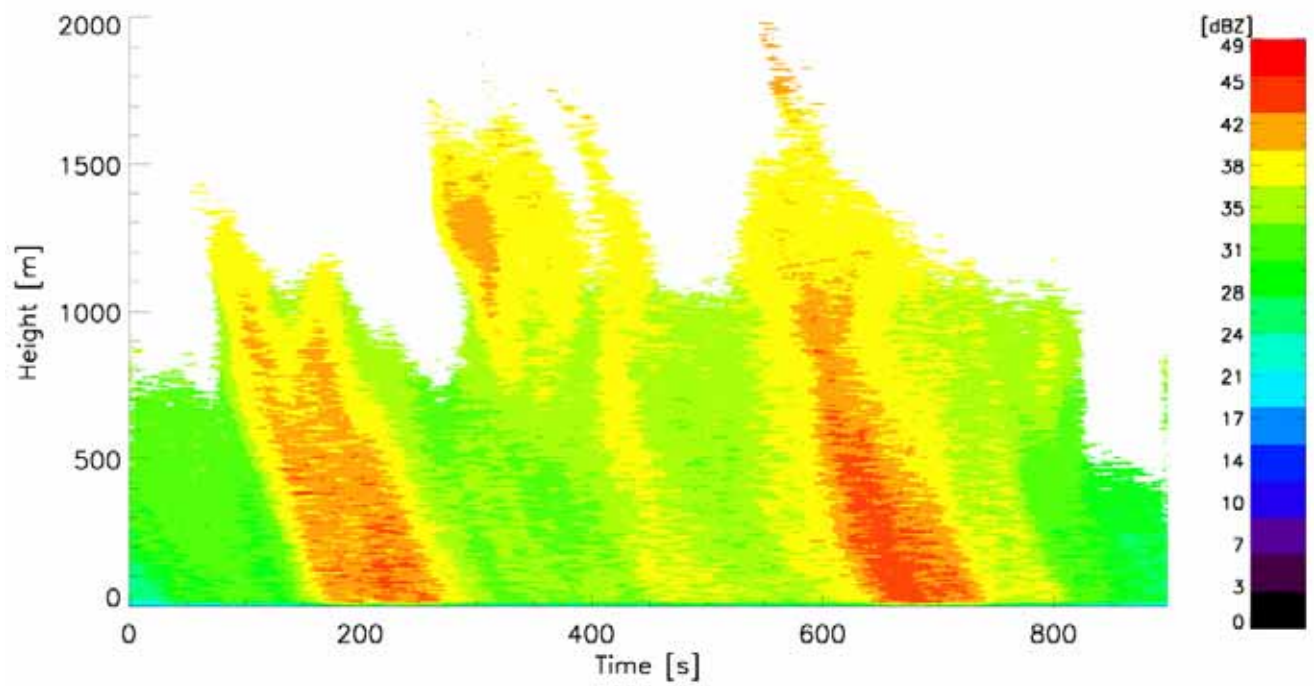


Figure 7. Same as Fig. 6 but for the interval from 10 to 25 minute

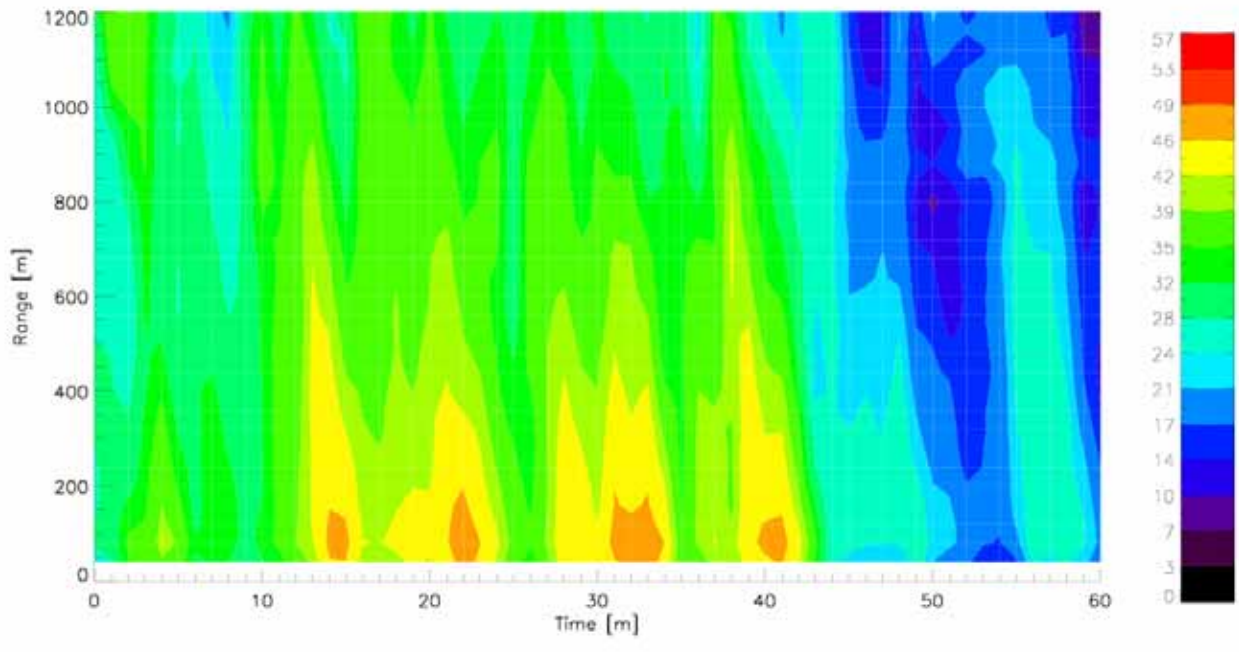


Figure 8 Vertical pointing observation by the Micro Rain Radar (METEK). The time of the observation is same as that in Figure 6. The radar is located 2 meters apart from our broad band radar.